NUCLEAR THEORY, Vol. 41 (2024)
eds. M. Gaidarov, N. Minkov, Heron Press, Sofia

Impact of the Nuclear Shape on the Soft Monopole Resonance in the Molybdenum Nuclei within Density-Dependent Meson-Exchange Theory and Quasiparticle Finite Amplitude Method

M. El Adri, **Y. El Bassem**, **A. El Batoul**, **M. Oulne**

High Energy Physics and Astrophysics Laboratory, Department of Physics, Faculty of Sciences Semlalia, Cadi Ayyad University, P.O.B. 2390, Marrakesh, Morocco

Abstract. This paper investigates the influence of nuclear deformation on the isoscalar giant monopole resonance (ISGMR) in the $^{98-102}$Mo isotopes using the quasiparticle finite amplitude method (QFAM) within the relativistic Hartree-Bogoliubov (RHB) framework. The study systematically explores the behavior of ISGMR under different axial and triaxial deformations, examining both spherical and deformed configurations. The calculations reveal shape coexistence and triaxial deformation effects, which significantly alter the ISGMR strength distributions. A detailed comparison with experimental data shows that accounting for nuclear deformation improves agreement, with deviations of less than 0.5 MeV. The findings emphasize the crucial role of deformation in understanding nuclear resonances, particularly in the context of soft monopole modes. The analysis of the $K = 0$ component of the ISGQR demonstrates notable monopole-quadrupole coupling, which contributes to the emergence of these soft monopole resonances.

1 Introduction

The isoscalar giant resonance [1,2], particularly its monopole component, offers crucial insights into nuclear dynamics and structure. It enables the determination of nuclear incompressibility, a key parameter in the nuclear equation of state. This collective excitation provides valuable information on nuclear matter properties under extreme conditions, aids in validating theoretical models, and has implications for understanding phenomena like neutron star structure and nuclear symmetry energy. Its study continues to be pivotal in bridging nuclear physics with astrophysics and advancing our comprehension of nuclear interactions.

The isovector giant dipole resonance (IVGDR) was first detected in 1947 using several techniques, such as photoabsorption, inelastic scattering, and γ-decay [3,4]. It wasn't until 1971-1972 that the isoscalar giant quadrupole resonance (ISGQR) was observed [5,6], followed by the discovery of the isoscalar giant monopole resonance (ISGMR) in 1977 [7]. From experimental data, empirical relationships for the energy of these resonances have been derived [8,9]. The ISGMR, in particular, is of special interest due to its link with the nuclear incompressibility factor K_0 [10,11].

This study explores nuclear excitation properties using microscopic approaches, primarily the Generator Coordinate Method (GCM) and Random Phase Approximation (RPA). While GCM mixes Hartree-Fock-Bogoliubov states, RPA offers computational efficiency and considers particle-hole excitations. RPA's evolution from condensed matter physics to nuclear systems led to advanced variants like QRPA and the Finite Amplitude Method. The research focuses on molybdenum isotopes, ideal for studying complex nuclear phenomena due to their structural features and deformation characteristics. It investigates resonances in the isoscalar monopole strength profile, considering nuclear deformation and neutron excess effects. Experimental findings reveal enhanced monopole strength across various nuclear regions, with some resonances linked to cluster modes or isoscalar monopole-quadrupole coupling. The study employs relativistic mean-field calculations with triaxial degrees of freedom to identify shape isomeric states and determine isoscalar giant monopole resonances at each equilibrium deformation. Using the QFAM method based on the axially deformed Relativistic Hartree-Bogoliubov approach, this research contributes to understanding nuclear deformation's influence on excitation modes in molybdenum isotopes. The structure of this article is as follows: In Section 2, we provide a brief summary of the approaches employed for our calculations. Section 3 contains the numerical specifics, information about the interactions utilized in our calculations, and a presentation, analysis, and discussion of the results obtained. Finally, in Section 4, we present the main conclusions drawn from our work.

2 Theoretical Framework

The Relativistic Hartree-Bogoliubov (RHB) framework offers a robust method for describing the decay, structural properties, and excited states of both spherical and deformed nuclei. In this approach, the nuclear state is represented by a generalized Slater determinant $|\Phi|$, which acts as a vacuum for independent quasiparticles. The quasiparticles are defined through a unitary Bogoliubov transformation, and the resulting Hartree-Bogoliubov wave functions, U and V, are derived from the RHB equation:

$$\begin{pmatrix} h_D - m - \lambda & \Delta \\ -\Delta^* & -h_D^* + m + \lambda \end{pmatrix} \begin{pmatrix} U_k \\ V_k \end{pmatrix} = E_k \begin{pmatrix} U_k \\ V_k \end{pmatrix} . \quad (1)$$

In this equation, the single-nucleon Dirac Hamiltonian is denoted as h_D, while Δ represents the pairing field, with U and V referring to Dirac spinors.

The quasiparticle finite amplitude method (QFAM) starts with the linear response equations [12], which serve as the foundation for exploring the response of the nuclear system to various perturbations

$$(E_\mu + E_\nu - \omega)\, X_{\mu\nu}(\omega) + \delta H^{20}_{\mu\nu}(\omega) = -F^{20}_{\mu\nu}, \tag{2}$$

$$(E_\mu + E_\nu + \omega)\, Y_{\mu\nu}(\omega) + \delta H^{02}_{\mu\nu}(\omega) = -F^{02}_{\mu\nu}, \tag{3}$$

In this formulation, E_μ and E_ν represent the quasiparticle energies, while $X_{\mu\nu}$ and $Y_{\mu\nu}$ denote the transition amplitudes. Specifically, $\mu\nu$ corresponds to the annihilation of two quasiparticles labeled as '02', and $\mu\nu$ refers to the creation of two quasiparticles labeled as '20'. Additionally, δH signifies the induced Hamiltonian resulting from the perturbation of the nuclear system by an external field F at a frequency ω. This framework facilitates the analysis of the system's response to external influences, allowing for a deeper understanding of its collective behavior.

Finally, the response function can be expressed as follows:

$$S_F(\hat{F}, \omega) = -\frac{1}{\pi} Im \sum_{\mu\nu} F^{20*}_{\mu\nu} X_{\mu\nu}(\omega) + F^{02*}_{\mu\nu} Y_{\mu\nu}(\omega), \tag{4}$$

Constrained Relativistic Hartree-Bogoliubov (RHB) calculations involve imposing constraints on both axial and triaxial quadrupole moments to construct a potential energy surface (PES) map. This approach employs the quadratic constrained method [13], where the goal is to minimize the function

$$\langle \hat{H} \rangle + \sum_{\mu=0,2} C_{2,\mu} (\langle \hat{Q}_{2\mu} \rangle - q_{2\mu})^2, \tag{5}$$

where $\langle \hat{H} \rangle$ represents the total energy of the system, and $\langle \hat{Q}_{2\mu} \rangle$ denotes the expectation value of the mass quadrupole operators. The function to be minimized can then be expressed as:

$$\hat{Q}_{20} = -(x^2 + y^2) + 2z^2,$$

and

$$\hat{Q}_{22} = x^2 - y^2, \tag{6}$$

The constrained value of the multipole moment is denoted as $q_{2\mu}$, while $C_{2\mu}$ represents the corresponding stiffness constant. The triaxial deformation parameter γ can be expressed in terms of the quadrupole moments $\hat{Q}_{20}$ and $\hat{Q}_{22}$ as follows:

$$\gamma = \arctan(\sqrt{2} \frac{\hat{Q}_{22}}{\hat{Q}_{20}}). \tag{7}$$

The quasiparticle finite amplitude method (QFAM) calculations have been conducted using the Relativistic Hartree-Bogoliubov (RHB) framework, constrained to various deformations parameterized by the axial quadrupole parameter β_2. This approach allows for the systematic exploration of different monopole resonances as the deformation of the nuclear system is varied, providing insights into both soft and cluster modes.

3 Numerical Details

The numerical approach followed in this analysis based on the methodologies suggested in Refs. [14, 15]. We utilize a full anisotropic triaxial-deformed harmonic oscillator basis, with $N_F = 14$ for fermions and $N_B = 20$ for bosons. The RHB equations and the nucleon equations of motion are solved within this basis, incorporating the covariant density-dependent meson-exchange functional DD-ME2 [16]. To effectively address pairing correlations in nuclei characterized by open shell closures, we apply the separable pairing force proposed by Tian et al. [17], which is implemented in coordinate space. Additionally, the smearing parameter is set to $\gamma/2 = 1.5$ MeV.

3.1 Ground-state deformation

Figure 1 shows the potential energy curves (PECs) of $^{98-102}$Mo isotopes calculated using the DD-ME2 functional, with the constraint on the axial deformation parameter β and triaxial parameter γ. These studied nuclei exhibit distinct deformation properties. The isotope ^{98}Mo exhibits triaxial deformation, with its potential energy surface (PES) indicating a single minimum at non-axial coordinates ($\beta_2 = 0.25$, $\gamma = 10°$), marking a clear deviation from simpler shapes.

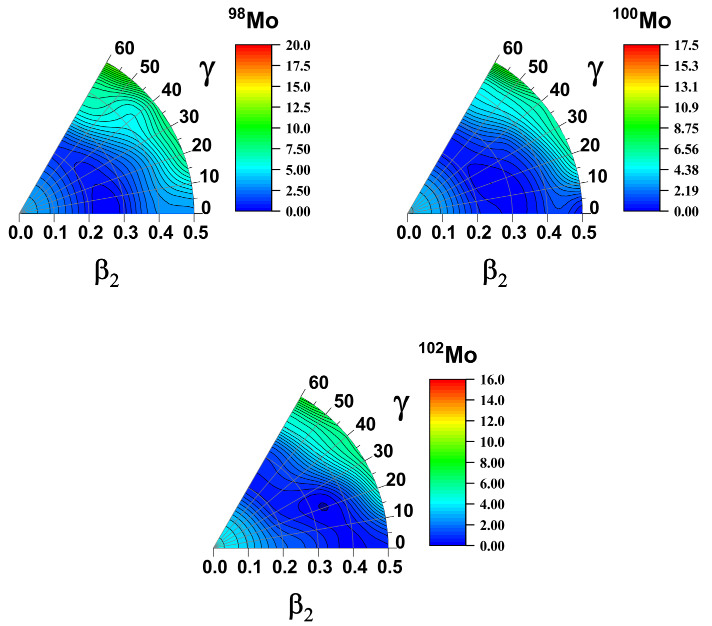

Figure 1. Potential energy curves obtained by constrained calculations with DD-ME2 functional.

Moving to ^{100}Mo, the PES reveals a more complex scenario, with triaxial deformation at ($\beta_2 = 0.25$, $\gamma = 20°$) accompanied by second minima at ($\beta_2 = 0.22$, $\gamma = 60°$), including a third significant minimum approximately 1 MeV above the ground state energy. This highlights the emergence of shape coexistence, where competing nuclear configurations are evident. Finally, in ^{102}Mo, triaxiality becomes even more pronounced, and an axial minimum appears in the oblate region, further suggesting the presence of shape coexistence. As deformation intensifies across these isotopes, the coexistence of multiple nuclear shapes becomes increasingly prominent, particularly in ^{100}Mo and ^{102}Mo.

3.2 QFAM strength evolutions

The isoscalar giant monopole resonances (ISGMR) for $^{98-102}$Mo isotopes have been calculated using the Quasiparticle Finite Amplitude Method (QFAM). These calculations, shown in Figure 2, are compared with experimental measurements. The analysis covers a frequency range up to 25 MeV, with calculations performed at 0.25 MeV intervals. The ISGMR profiles were determined under two conditions: assuming a spherical nuclear shape and using the exact shape isomeric states. The results show good agreement with experimental data, with discrepancies generally less than 0.5 MeV. Notably, the agreement improves when nuclear deformation effects are considered in the calculations.

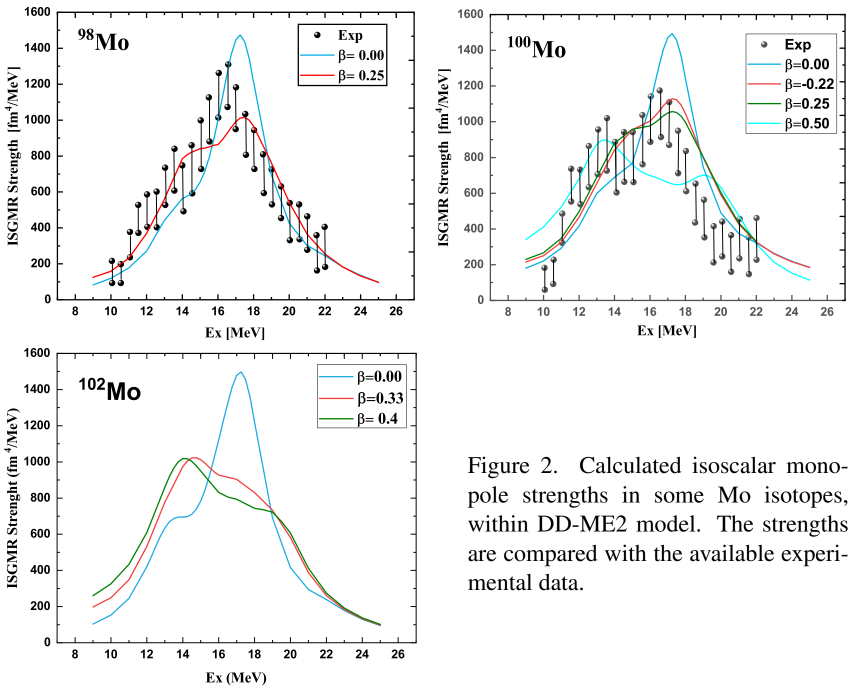

Figure 2. Calculated isoscalar monopole strengths in some Mo isotopes, within DD-ME2 model. The strengths are compared with the available experimental data.

The analysis of $^{98-102}$Mo reveals a consistent main ISGMR peak around 17 MeV in spherical configurations, with an increasingly prominent low-energy shoulder as neutron number increases. When deformation is considered, the main peak broadens and the low-energy shoulder becomes more pronounced, particularly in heavier isotopes. The interplay between the main peak and shoulder suggests a gradual exchange of positions with increasing mass number. ^{100}Mo, being the most deformed, exhibits a sharp main peak at 14.5 MeV for oblate deformations, accompanied by a weak secondary shoulder around 22.5 MeV. This isotopic chains demonstrates the significant influence of both nuclear deformation and neutron excess on the ISGMR strength distribution, especially evident in the evolution of low-energy shoulders and the sensitivity to the deformation parameter β_2.

The observed splitting of the ISGMR into two peaks can be attributed to the coupling between monopole and K=0 component quadrupole modes, a characteristic feature of deformed nuclei with non-zero β_2. To investigate this correlation, the K=0 component of ISGQR strength was analyzed using the DD-ME2 model. The results, presented in Figure 3, reveal a clear alignment between ISGQR peaks and monopole strength shoulders for $\beta_2 > 0$ (prolate configurations). However, this alignment is absent for $\beta_2 < 0$ (oblate configurations), indicating a selective coupling mechanism.

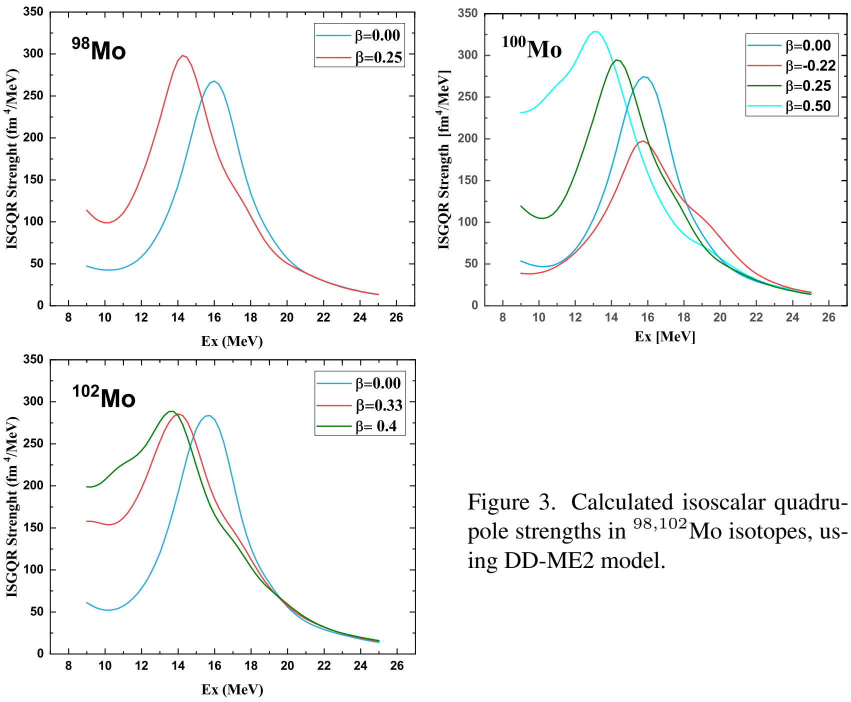

Figure 3. Calculated isoscalar quadrupole strengths in ^{98,102}Mo isotopes, using DD-ME2 model.

This pattern mirrors findings from previous studies on zirconium isotopes, reinforcing the observation that monopole-quadrupole coupling occurs predominantly in prolate configurations, while being notably absent in oblate cases. The phenomenon can be understood through the lens of angular momentum behavior in axially deformed nuclei. Unlike spherical nuclei where total intrinsic angular momentum defines intrinsic states, axially deformed nuclei rely on the angular momentum projection K as the sole good quantum number for intrinsic excited states.

Consequently, any non-zero quadrupole deformation theoretically permits mixing of monopole and quadrupole modes in K=0 intrinsic states. In the case of Mo isotopes, this mixing manifests exclusively in prolate configurations. The resulting quadrupole peak, induced by monopole-quadrupole coupling, appears in the isoscalar monopole strength function at an energy typical for the E2 ISGQR centroid position. Notably, the intensity of this shoulder is directly proportional to the strength of the monopole-quadrupole mixing, which increases with greater quadrupole deformation .

4 Conclusion

This study examined isoscalar giant monopole resonances (ISGMR) in molybdenum isotopes (^{98,102}Mo) using the quasiparticle finite amplitude method within a relativistic framework. It revealed shape coexistence in heavier isotopes, consistent ISGMR peaks around 17 MeV in spherical configurations, and increasingly prominent low-energy shoulders with increasing neutron number. Nuclear deformation effects enhanced these features and improved agreement with experimental data. The research also demonstrated monopole-quadrupole coupling, predominantly in prolate configurations. These findings contribute significantly to our understanding of nuclear structure and dynamics, emphasizing the importance of considering deformation in nuclear resonance studies and illuminating the complex relationship between nuclear shape and excitation modes.

References

[1] P.F. Bortignon, A. Bracco, R.A. Broglia, "*Giant Resonances. Nuclear Structure at Finite Temperature*", (CRC Press, 2019).

[2] M. Harakeh, A. Woude, "*Giant Resonances: Fundamental High-frequency Modes of Nuclear Excitation*", (Oxford Studies in Nuclear Physics, 2001).

[3] G.C. Baldwin, G.S. Klaiber, *Phys. Rev.* **71** (1974) 554.

[4] L. Donaldson, et al., *Phys. Lett. B* **776** (2018) 133.

[5] R. Pitthan, T. Walcher, *Phys. Lett. B* **36** (1971) 563-564.

[6] M.B. Lewis, F.E. Bertrand, *Nucl. Phys. A* **196** (1971) 2

[7] M.N. Harakeh, et al., *Phys. Rev. Lett.* **38** (1971) 676.

[8] S. Fukuda, Y. Torizuka, *Phys. Rev. Lett.* **29** (1972) 1109.

[9] B.L. Berman, S.C. Fultz, *Rev. Mod. Phys.* **47** (1972) 713.

[10] J.P. Blaizot, et al., *Nucl. Phys. A* **591** (1995) 435.
[11] U. Garg, G. Coló, *Prog. Part. Nucl. Phys.* **101** (2018) 95.
[12] A. Bjelčić, T. Nikšić, *Comp. Phys. Commun.* **253** (2020) 107184.
[13] P. Ring, P. Schuck, "*The Nuclear Many-Body Problem*", (Springer Science and Business Media, 2004).
[14] M. El Adri, M. Oulne, *Eur. Phys. J. Plus* **135** (2020) 268.
[15] M. El Adri, M. Oulne, *IJMPE* **29** (2020) 2050089.
[16] G.A. Lalazissis, T. Nikšić, D. Vretenar, P. Ring, *Phys. Rev. C* **71** (2005) 024312.
[17] Y. Tian, Z.Y. Ma, P. Ring, *Phys. Lett. B* **676** (2009) 44-50.